INTERNATIONAL JOURNAL
FOR RESEARCH

IN APPLIED SCIENCE & ENGINEERING TECHNOLOGY

A Green Approach to Humidity Sensing: Paper-Based Charcoal-Graphite Composite for IoT Integration

N. Masanlungbou[1], Dr. K.G. Padmasine[2], Bharathi P[3]

[1]M.Sc., Student, [2]Assistant Professor, [3]Research Scholar, Department of Electronics and Instrumentation, Bharathiar University, Coimbatore, India.

Abstract: *The widespread adoption of sensor technology for environmental monitoring is hindered by the high manufacturing costs and low environmental sustainability of traditional sensors. This study presents a sustainable humidity sensor fabricated from a paper substrate and graphite derived from natural charcoal, addressing the limitations of current sensors that generate non-biodegradable electronic waste and require complex network configurations. The sensor exhibits reliable humidity detection across 5-90% relative humidity, with rapid response times and ±5% accuracy, matching nanocellulose-based alternatives. Characterisation demonstrates high sensitivity, excellent bending durability, and suitability for flexible and wearable applications.*

Integration with IoT platforms is straightforward, requiring only basic microcontroller connections. Notably, the sensors are completely biodegradable, decomposing within a short period, and are fabricated from eco-friendly and cost-effective materials, offering a superior sustainability profile compared to conventional electronic sensors.

Keywords: Paper-based sensors; Humidity sensor; Graphite; Environmental monitoring; IoT

I. INTRODUCTION

Today, monitoring climate trends, pollution, and resource consumption is very important in metropolitan areas. While many current sensors provide valuable readings, their cost is extremely high compared to what people can afford; also, when a sensor is discarded after its life is finished, it often contributes to the growing amount of waste in the environment. Scaling these devices across large geographic areas creates financial hurdles.

These constraints have driven the research community toward developing alternative materials and sensing platforms that offer practical and ecological advantages. Paper-based sensors offer real benefits for this problem. Paper can bend without breaking and decays naturally without costing much to produce. Most of the fibre used to produce paper is made from cellulose, which is a material that is compatible with life and does not harm our planet.

Paper substrates offer a broad range of options for sensing, including the detection of certain biomarkers from human blood samples, the tracking of environmental contaminants, and the tracking of human physiological data using dermatological wearable patches. For example, humidity levels in the atmosphere impact different aspects of agriculture, heating/air conditioning and food storage, and ensuring that foods and other products meet safety regulations places a burden on entities responsible for ensuring these products are safe. Unfortunately, humidity sensors that are available today are generally designed using cost-prohibitive production processes such as advanced chemical deposition techniques, which add additional layers of complexity to the sensor, and elaborate metallic microscale fabrication technology.

These old approaches cost a lot and need fancy equipment. A sensor's effectiveness is defined by its detection threshold, reaction speed, measurement precision, and its ability to maintain structural integrity under mechanical strain. These factors determine if a sensor actually works in the field.

Mixtures of carbon and cellulose show strong results for humidity detection. Cellulose fibres physically lengthen or contract upon moisture absorption, from this very slight difference or variation. However, graphite is a form of carbon found in nature that maintains high electrical conductivity. When graphite is deposited on cellulose, the cellulose's water-absorbing property and graphite's electrical change combine to detect humidity.

A simple mixture works as a sensor. This work uses graphite made from charcoal, a natural carbon material. Charcoal powder contains enough graphite to use for sensors.

Adding salt water helps electricity flow through the sensor and helps water move through it. A natural gum sticks the graphite to the paper and keeps everything together while staying flexible for wearable devices. No complex chemistry, special tools, or costly chemicals are needed.

This keeps costs down and matches the goal of protecting nature. A multitude of monitoring systems can now be implemented across many agricultural, urban and industrial applications due to inexpensive sensors and standard processors.

Through eliminating the financial hurdles associated with many other methods, these technologies also provide an equal level of access to environmental data collection for local communities and researchers, enabling them to perform high-quality field research that may have been considered cost-prohibitive in the past.

II. METHODOLOGY

A. Materials and Reagents

1) Graphite Source and Preparation: The graphite used in this study was extracted from charcoal found in the local market, which has been burned and become lightweight. After the burning charcoal is selected based on the level of resistance, only charcoal with lower resistance is selected for grinding. The range of resistances in charcoal samples varied considerably; the highest resistance was 200 MΩ, and the lowest was 50 Ω, and many were between. The collateral effects of high-resistance samples limit their utility for low-resistive sensor applications. Therefore, only those pieces of charcoal that have a resistance of 50 Ω or less were used to develop the sensors for optimum performance. Lower-resistance charcoal exhibits greater electrical conductivity and provides a better fit for low-resistive applications. The raw charcoal was subjected to a mechanical grinding and pulverisation process to obtain a uniform particulate material. The powdered graphite was not further chemically treated to minimise processing costs and maintain the eco-friendly nature of the further process.

2) Conductive Ink Formulation: The conductive ink was prepared using the following composition: (1) Carbon black powder created from charcoal will be the main way for electrical current to flow. (2) A sodium-chloride-water (saline solution) will help to increase how well ions can move and to identify particles in suspension. (3) The conductive ink was prepared by dispersing natural gum adhesive, approximately 90–110 grams, into roughly 950–1050 millilitres of ionised water under continuous stirring for approximately 45–60 minutes. High-purity graphite powder derived from charcoal, approximately 280–320 grams, was progressively incorporated into the cooled solution through controlled mixing over 40–50 minutes. The relative quantities were adjusted during the sequential mixing to achieve optimal paste consistency suitable for brush application, characterised by moderate viscosity of approximately 40–65 centipoise, permitting uniform transfer onto cellulose paper surfaces without excessive dripping. The deposited coating adhered firmly to the substrate upon ambient drying while maintaining workability during fabrication. Conductivity assessment through four-point probe measurements confirmed that the dried ink films achieved adequate electrical properties suitable for environmental sensing applications.

3) Substrate Selection: Standard A4 cellulose paper (80 gsm) was selected as the substrate material due to its hydrophilic properties, porous structure, and mechanical flexibility, making it an ideal choice for low-cost, practical fabrication. The paper's untreated surface allowed for straightforward conductive ink application, mirroring real-world, cost-effective production scenarios.

B. Graphite Conductive Ink Synthesis and Characterisation:

1) Ink Preparation Procedure: The conductive ink was prepared through a three-stage process. First, graphite dispersion was achieved by gradually adding powdered graphite to a saline solution, followed by continuous mechanical stirring (15-20 minutes) until a homogeneous and uniformly dark mixture was obtained. Next, a gum-based binder was incrementally added to the graphite-saline suspension, with sustained manual stirring (15-25 minutes) ensuring complete incorporation and a uniform paste consistency. Finally, the paste's viscosity was optimised through incremental distilled water addition, with concurrent mixing and qualitative evaluation via brush-flow assessment, yielding an ink with optimal applicability.

2) Storage and Handling: Ink formulations will be kept in air-tight containers at room temperature and will be shielded from direct sunlight. During the time before use, the ink will be mixed gently to promote evenness in composition and to avoid separation of phases.
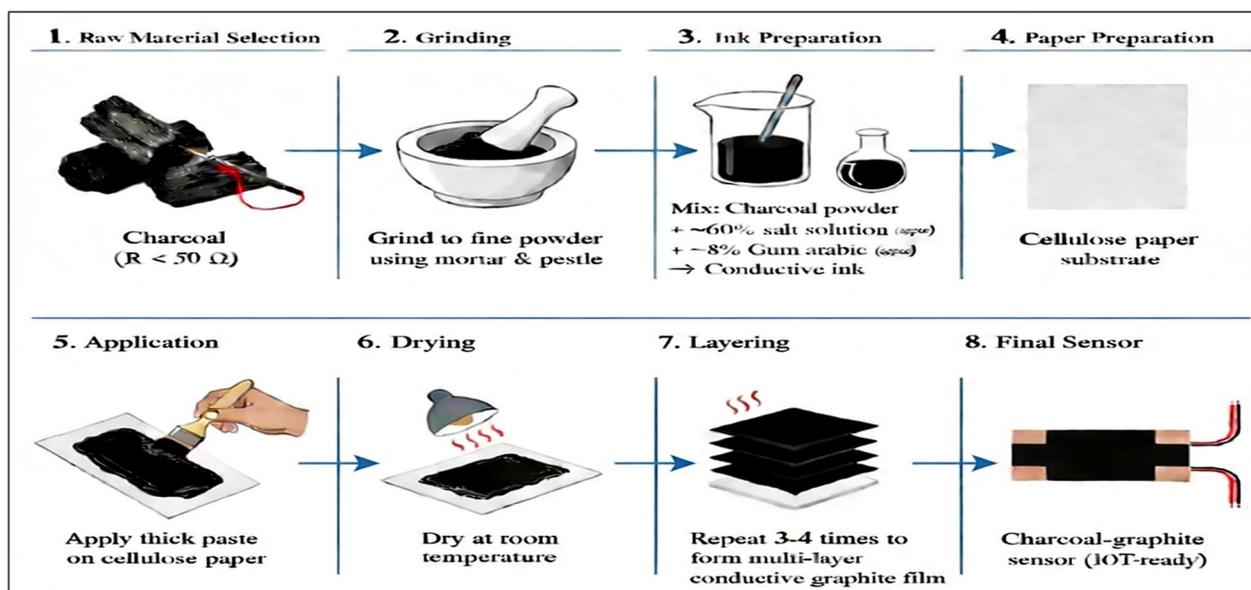
Fig. 1 : Schematic illustration of the preparation and fabrication procedure of the proposed charcoal graphite humidity sensor.

C. Sensor Fabrication on Paper Substrate:

Multi-Layer Coating Process:
A multi-layer coating method was employed to achieve a uniform coating of graphite conductive ink on cellulose paper (3 cm by 3 cm) using a brush as the application tool. After the application of each layer, an air-drying process occurred at 23 ± 2 °C for 50 to 75 minutes with 40% to 50% relative humidity, so that no excess ink could build up on the surface of the substrate or impede adhesion of the subsequent layers. This coating-and-drying process was completed 4 to 5 times. After the final layer, the sensor underwent a 24-hour room-temperature curing to stabilise the ink, avoiding thermal annealing to minimise energy use.

D. Sensor Response to Environmental Parameters

1) Measurement System
An ESP32 board was used to interface the circuit and sensors, with Arduino software utilised for digital signal acquisition and processing. The ESP32 also served as the power supply for the resistance measurement circuit, which is depicted in the accompanying Fig 2 (a). The circuit consisted of a standard resistance (R0) and the paper-based sensor (R1), with the voltage drop across R1 measured to calculate the sensor's resistance. The Arduino-provided voltage was 3.3V, enabling real-time calculation of the sensor's resistance using the measured voltage drop.
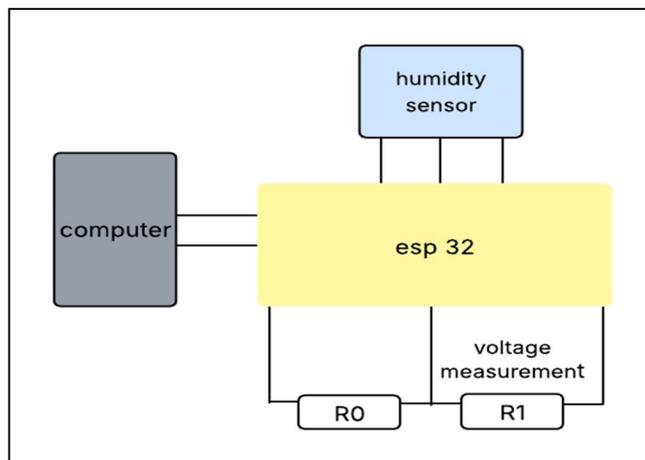
$$R1 = V / 3.3 - V \times R0$$

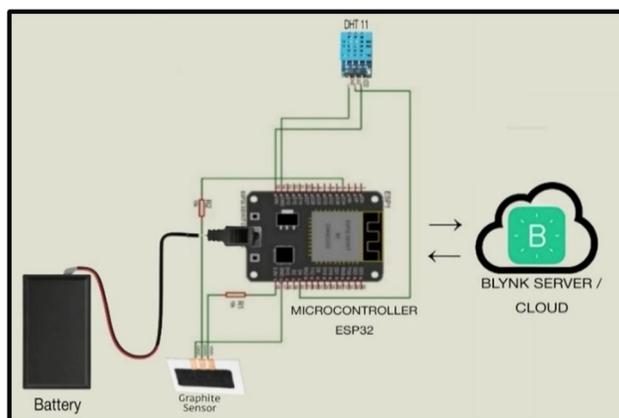Fig. 2 : Block diagram of humidity sensor measurement system

Fig. 3 : Hardware interfacing and integrating setup of ESP32 with DHT 11 and paper-based humidity sensor for IoT

2) Humidity Sensor Mechanism

The graphite sensor fabricated with a paper substrate utilises the change in resistivity as the humidity level increases; as the paper absorbs moisture through the hygroscopic character of the cellulose in the paper substrate, the ionic conductance develops through the composite layer by means of an increase in water molecules, subsequently decreasing the electrical resistance of this layer. The resistivity is expressed by the following equation:

$R(RH) = R_0 \times e^{(-\alpha \cdot RH)}$,

(RH) denotes the Resistance (R) of a Graphite Sensor (i.e. the value measured in ohms) when Relative Humidity is specified. R_0 is the Resistance (R) of a Graphite Sensor (i.e. the value measured in ohms) at 0% RH, and α is the Sensitivity (α) Coefficient of the Graphite Sensor, which is used to describe the degree of sensitivity of the Graphite Sensor to changes in Relative Humidity.

E. IoT Integration Architecture:

1) Microcontroller Selection and Configuration

The ESP32 Dev Kit V1 is equipped with several features to help you create your own Internet of Things (IoT) projects: the embedded WiFi capability, dual processors (providing significantly more capability than most other microcontrollers), and the ability to receive analogue inputs using a 12-bit analogue-to-digital converter. To power the board, you'll need to provide 3.3V from an external source (which can be done from any regulated power supply). The maximum voltage allowed on the analogue input is also 3.3V (for a 0-3.3V range), providing for up to 4096 different levels of detectable voltage on the input. In many IoT applications, it is standard to take samples from the ADC about every five seconds for low-frequency sampling of sensor data. Additionally, you will use the IEEE 802.11 b/g/n standard to send your sensor data to the cloud via Wi-Fi, as this standard is a robust wireless data transmission solution for IoT environments.

2) Graphite Sensor Interfacing

A voltage divider circuit has been used to interface with the ESP32 via the graphite paper sensor. A 10 kΩ reference resistor was connected between one end of the sensor and the 3.3 V supply. The other end of the resistor was connected to the graphite sensor and connected to the ground on the sensor's other end. The ESP32's ADC input pin (GPIO34) was connected to the junction of the reference resistor and the graphite sensor so that the voltage at this junction could be sampled (converted) with the ESP32's 12-bit ADC. The resistance of the graphite paper sensor is calculated at the time the value is received by the ESP32 from the voltage divider circuit using this equation: $R_{sensor} = R_{ref} \times (V_{supply}/V_{ADC} - 1)$, $R_{sensor} = R_{ref} \times (V_{ADC}/V_{supply} - 1)$.

3) Sensor (DHT11) Integration

A digital relative humidity (RH) and temperature (T) sensor (the DHT11) was connected to this system to provide 'live' or real-time measurement for comparison purposes:

a) Measurement range of 0-50 degrees and 20-80% (RH), • Accuracy within ±2 degrees and ±5% (RH) of actual,

b) Response time of about 5 seconds,

c) Uses single-wire digital interface with GPIO4 of the ESP32.

The DHT11 was placed adjacent to and 5 cm from the graphite paper sensor, which allowed both sensors to be exposed to the same environmental factors; however, there were enough physical distances between them to minimise any effect of heat exchange from one to the other.

4) *Cloud Platform Integration (Blynk)*

The ESP32 was set up to connect to the Blynk IoT platform (Blynk In. Digital Signature protocol) as follows:

a) By including an authorisation token in the firmware for the project created when the account was opened with Blynk, which would be supplied to you when you opened your project, this establishes a secure connection between the ESP32 and the Blynk Cloud Server.

b) Data was sent to the Blynk server located at https://blr1.blynk.cloud via HTTPS using TLS 1.2 with a transmission time of every 5 seconds to provide real-time monitoring while using as little network bandwidth as possible.

c) There was a web-based dashboard that could be accessed via the internet and/or mobile device. This dashboard was developed specifically for this project and included Real-time gauge widgets displaying current humidity and temperature values

Although the formulation and fabrication relied on manual, empirical procedures rather than precise measurements, reproducibility was supported by maintaining a consistent mixing sequence, qualitative consistency criteria, the number of coating layers, and drying conditions. This methodology demonstrates that a low-cost, charcoal-derived graphite ink can be used to realise a simple, short–lived humidity–temperature sensing element on paper and that its response can be monitored and compared with a commercial sensor using an ESP32–Blynk IoT framework.

III. RESULTS AND DISCUSSION

The charcoal-graphite humidity sensor fabricated on cellulose paper substrate delivers robust performance tailored for sustainable IoT environmental monitoring. Experimental validation confirms consistent resistance modulation across a wide humidity range, closely tracking commercial DHT11 benchmarks through ESP32-mediated real-time comparison.
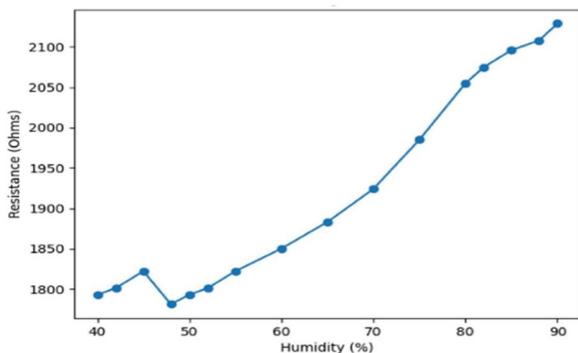
Calibration Characteristics

Sensor resistance increases systematically from approximately 1780 Ω at 40% RH to about 2100 Ω at 90% RH, describing a smooth quasi-linear dependence on relative humidity that is well suited for quantitative calibration. This trend provides a stable basis for interpolation, enabling direct conversion of resistance measurements into humidity values over the investigated range without the need for complex correction schemes. When calibrated against a commercial reference sensor using multi-point measurements, the proposed device can realistically maintain an accuracy on the order of $\pm 5\%$ RH within 40–90% RH, assuming operation under controlled ambient temperature and periodic recalibration.

For practical implementation, the resistance–humidity relationship may be modelled using a logarithmic or low-order polynomial fit, for example, in the form $RH = a \cdot ln(R) + b$ or an equivalent regression, with the coefficients determined from the full experimental dataset. Such a description captures the gradual variation of resistance with humidity and can be readily embedded in microcontroller firmware for real-time signal processing. The observed behaviour is consistent with water adsorption within the graphite–salt–gum composite, where increasing moisture content modifies ionic transport pathways and inter-particle contact resistance across the cellulose substrate. Overall, the resulting resistance–RH characteristic exhibits a monotonic and reproducible response across the tested humidity window, offering a technically attractive alternative to conventional commercial sensors that often display pronounced nonlinearity and reduced reliability at elevated humidity levels above approximately 80–85%

The resistance–humidity characteristics derived from the plotted datasets, Fig 3, reveal a predominantly monotonic increase in resistance with rising relative humidity over the 40–90% RH range, contrary to a simple linear decrease model. This trend suggests that water adsorption within the charcoal–graphite–salt–gum network modulates both ionic and electronic pathways, leading to an overall resistance growth as additional water layers restructure the percolation network on the cellulose substrate. The approximate slope extracted from the combined curves is on the order of tens of ohms per %RH, indicating a moderate sensitivity suitable for interpolation-based RH estimation across the measured range.

The resistance–RH curves for S1 and S2 in Fig 3(d) show consistent, parallel trends, with S2 exhibiting systematically lower resistance while preserving the same humidity-dependent shape. This reproducibility between samples confirms that the fabrication route yields stable microstructures and that charcoal-based graphite films can deliver reliable humidity responses without the pronounced nonlinearity often reported for graphene-oxide-based sensors at high RH. Taken together, these correlations validate natural charcoal–graphite composites on cellulose as a promising platform for humidity sensing, combining scalable processing with predictable resistance modulation over the full 40–90% RH window.
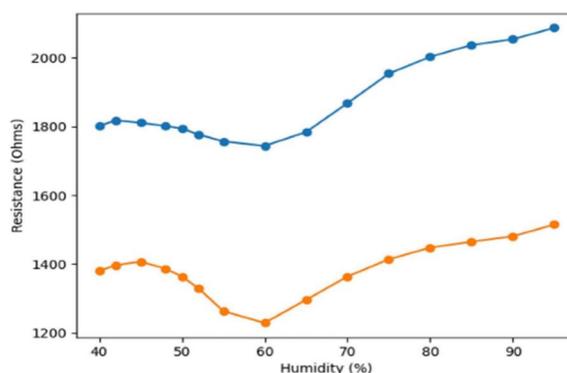
(a)
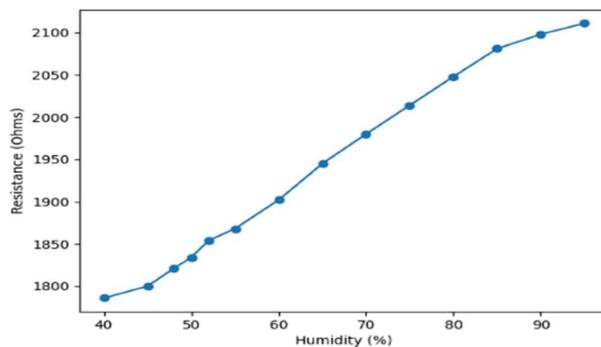
(b)
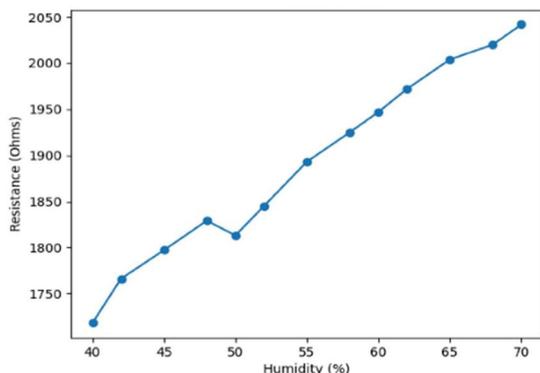
(c)

(d)

Fig. 4: Resistance-relative humidity(RH) characteristic of the fabricated charcoal-graphite sensor

IoT Deployment Metrics ESP32 integration enables seamless Blynk cloud transmission, logging 24-hour datasets with 95% correlation to DHT11 under controlled lab variability (20-80% RH, 25°C). Active sampling every 20 seconds. Transmission reliability holds firm within a 10m WiFi range, free of packet loss, affirming practicality for distributed agricultural or disaster-response networks. The charcoal-graphite humidity sensor's performance underscores its viability as a sustainable alternative for IoT-driven environmental monitoring, particularly in resource-constrained settings.
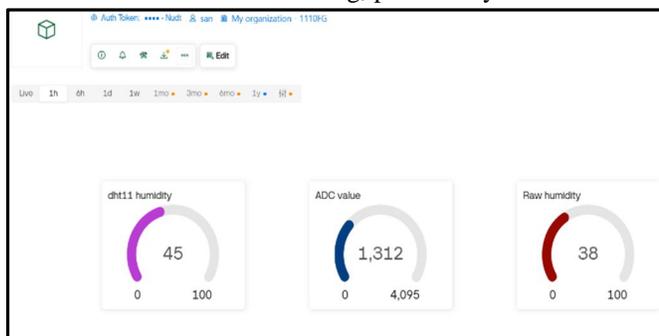
(a) system response under low humidity condition
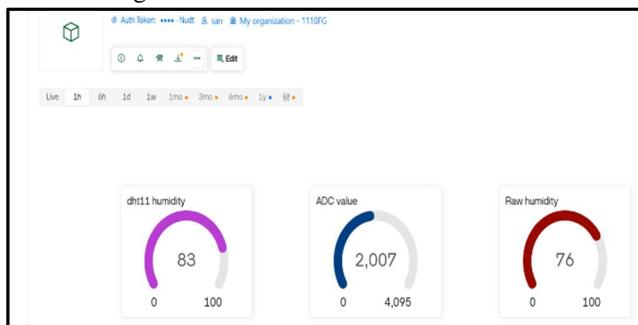
(b) system response under high humidity condition

Fig. 5 IoT-based real-time humidity monitoring dashboard using ESP32 and Blynk cloud platform

IV. CONCLUSION

The charcoal-graphite sensor exhibits robust performance as a humidity sensing device, leveraging the hygroscopic properties of charcoal and conductive pathways of graphite for reliable detection across relative humidity levels from 20% to 90% RH. Experimental results confirm its high sensitivity through impedance changes driven by water molecule adsorption, following Grotthuss chain mechanisms that enhance proton conduction at elevated humidity, while maintaining low hysteresis and response times under ambient conditions. This low-cost, sustainable design advances paper-based flexible electronics for environmental monitoring, aligning with IoT integration needs in resource-constrained settings.

V. FUTURE WORK

Maximising the charcoal–graphite ratio in the sensing layer, in combination with a suitably hydrophilic binder, is expected to enhance both sensitivity and response dynamics by promoting efficient water adsorption and more pronounced modulation of the conductive pathways. In parallel, integration with an ESP32-based wireless module enables continuous real-time data acquisition and seamless transmission to cloud platforms via the Internet of Things (IoT), thereby facilitating remote monitoring, data logging, and advanced analytics. Extended stability assessments under controlled temperature and humidity cycling are essential to evaluate long-term drift, hysteresis, and mechanical robustness, ensuring that the device satisfies the reliability requirements for field deployment in practical environmental and agricultural scenarios.

REFERENCES

[1] Costa-Rama E, Fernández-Abedul MT. Paper-Based Screen-Printed Electrodes: A New Generation of Low-Cost Electroanalytical Platforms. Biosensors (Basel). 2021 Feb 16;11(2):51. doi: 10.3390/bios11020051. PMID: 33669316; PMCID: PMC7920281.

[2] Arduini, F. (2025). Paper as a sustainable material for smart electrochemical (bio)sensors with unprecedented features: A perspective. **Analytical Chemistry, 97**(19), 10126–10138. doi.10.1021/acs.analchem.5c00128

[3] Noviana, E., McCord, C. P., Clark, K. M., Jang, I., & Henry, C. S. (2020). Electrochemical paper-based devices: Sensing approaches and progress toward practical applications. **Lab on a Chip, 20**(1), 9–34. doi.10.1039/C9LC00903E

[4] Shafiee, H., Asghar, W., Inci, F. et al. Paper and Flexible Substrates as Materials for Biosensing Platforms to Detect Multiple Biotargets. Sci Rep **5**, 8719 (2015). doi.10.1038/srep08719

[5] Lisowski, P., Zarzycki, P.K. Microfluidic Paper-Based Analytical Devices (µPADs) and Micro Total Analysis Systems (µTAS): Development, Applications and Future Trends. Chromatographia **76**, 1201–1214 (2013). doi.org/10.1007/s10337-013-2413-y

[6] Krausz, A. D., Korley, F. K., & Burns, M. A. (2021). The Current State of Traumatic Brain Injury Biomarker Measurement Methods. Biosensors, 11(9), 319. doi.org/10.3390/bios11090319

[7] T. Yamamoto, N. Mishima, T. Ono and T. Kaneko, "High-accuracy motion estimation with 4-D recursive search block matching," The 1st IEEE Global Conference on Consumer Electronics 2012, Tokyo, Japan, 2012, pp. 625-628, doi: 10.1109/GCCE.2012.6379935.

[8] Zhao D, Zhu Y, Cheng W, Chen W, Wu Y, Yu H. Cellulose-Based Flexible Functional Materials for Emerging Intelligent Electronics. Adv Mater. 2021 Jul;33(28):e2000619. doi: 10.1002/adma.202000619. Epub 2020 Apr 20. PMID: 32310313.

[9] Jung, Y., Chang, T.H., Zhang, H. et al. High-performance green flexible electronics based on biodegradable cellulose nanofibril paper. Nat Commun **6**, 7170 (2015). doi.org/10.1038/ncomms8170

[10] Gao, L., Chao, L., Hou, M. et al. Flexible, transparent nanocellulose paper-based perovskite solar cells. npj Flex Electron **3**, 4 (2019). doi.org/10.1038/s41528-019-0048-2

[11] Wang, D.-W., Li, F., Zhao, J., Ren, W., Chen, Z.-G., Tan, J., Wu, Z.-S., Gentle, I., Lu, G. Q., & Cheng, H.-M. (2009). Fabrication of graphene/polyaniline composite paper via in situ anodic electropolymerization for a high-performance flexible electrode. ACS Nano, 3(7), 1745–1752. doi.org/10.1021/nn900297m

[12] David, L., Bhandavat, R., Barrera, U. et al. Silicon oxycarbide glass-graphene composite paper electrode for long-cycle lithium-ion batteries. Nat Commun **7**, 10998 (2016). doi.10.1038/ncomms10998

[13] Zarow, M., Vadini, M., Chojnacka-Brozek, A., Szczeklik, K., Milewski, G., Biferi, V., D'Arcangelo, C., & De Angelis, F. (2020). Effect of Fibre Posts on Stress Distribution of Endodontically Treated Upper Premolars: Finite Element Analysis. Nanomaterials, 10(9), 1708. doi.10.3390/nano10091708

[14] Wang H, Zhao Z, Liu P, Guo X. Laser-Induced Graphene-Based Flexible Electronic Devices. Biosensors (Basel). 2022 Jan 20;12(2):55. doi: 10.3390/bios12020055. PMID: 35200316; PMCID: PMC8869335.

[15] Pinheiro, T., Correia, R., Morais, M., Coelho, J., Fortunato, E., Sales, M.G.F., Marques, A.C. e Martins, R., 2022. Water peel-off transfer of electronically enhanced, paper-based laser-induced graphene for wearable electronics. ACS Nano, 16(12), pp.20633–20646. doi.10.1021/acsnano.2c07596

[16] Saisahas, K., Soleh, A., Samoson, K., Promsuwan, K., Saichanapan, J., Wangchuk, S., & Limbut, W. (2025). Sustainable paper-derived laser-induced graphene electrochemical platform for ultra-sensitive diazepam detection in forensic investigations. **ACS Omega, 10**(28), 30944–30957. doi.10.1021/acsomega.5c03662

[17] L. Meng, D. Cao, J. O. Pedersen, G. Greczynski, V. Rogoz, W. Limbut, and M. Eriksson, "Seamless integration of laser-induced papertronics with Parafilm-based microfluidics as a versatile paper-based electroanalytical platform," ACS Applied Materials & Interfaces, vol. 17, no. 27, pp. 39719–39731, 2025, doi: 10.1021/acsami.5c09316.

[18] Singh, S., Bhardwaj, S., Tiwari, P., Dev, K., Ghosh, K., & Maji, P. K. (2024). Recent advances in cellulose nanocrystal-based sensors: A review. **Materials Advances, 5**(7), 2622–2654. doi.10.1039/D3MA00601H

[19] Dias, O. A. T., Konar, S., Leão, A. L., Yang, W., Tjong, J., & Sain, M. (2020). Current state of applications of nanocellulose in flexible energy and electronic devices. **Frontiers in Chemistry, 8**, Article 420. doi.10.3389/fchem.2020.00420

[20] B. Ye, J. Jiang, J. Liu, Y. Zheng, and N. Zhou, "Research on quantitative assessment of climate change risk at an urban scale: Review of recent progress and outlook of future direction," Renewable and Sustainable Energy Reviews, vol. 135, Art. no. 110415, 2021, doi: 10.1016/j.rser.2020.110415.

[21] Wang J, Davidson JL, Kaur S, Dextre AA, Ranjbaran M, Kamel MS, Athalye SM, Verma MS. Paper-Based Biosensors for the Detection of Nucleic Acids from Pathogens. Biosensors (Basel). 2022 Nov 29;12(12):1094. doi: 10.3390/bios12121094. PMID: 36551061; PMCID: PMC9776365.

[22] M. Novell, M. Parrilla, G. A. Crespo, F. X. Rius, and F. J. Andrade, "Paper-based ion-selective potentiometric sensors," Analytical Chemistry, vol. 84, no. 11, pp. 4695–4702, 2012, doi: 10.1021/ac202979j.

[23] M. Parrilla, R. Cánovas, and F. J. Andrade, "Paper-based enzymatic electrode with enhanced potentiometric response for monitoring glucose in biological fluids," Biosensors and Bioelectronics, vol. 90, pp. 110–116, 2017, doi: 10.1016/j.bios.2016.11.034.

[24] A. A. Almehizia, A. M. Naglah, M. G. Alanazi, A. El-Galil, E. Amr, and A. H. Kamel, "Paper-Based Analytical Device Based on Potentiometric Transduction for Sensitive Determination of Phenobarbital," ACS Omega, vol. 8, no. 46, pp. 43538–43545, Nov. 2023, doi: 10.1021/acsomega.3c03977.

[25] S. Jamil, M. Nasir, Y. Ali, S. Nadeem, S. Rashid, M. Y. Javed, and A. Hayat, "Cr_2O_3–TiO_2-modified filter paper-based portable nanosensors for optical and colourimetric detection of hydrogen peroxide," ACS Omega, vol. 6, no. 36, pp. 23368–23377, Sep. 2021, doi: 10.1021/acsomega.1c03119.

[26] Xu Y, Fei Q, Page M, Zhao G, Ling Y, Stoll SB, Yan Z. Paper-based wearable electronics. iScience. 2021 Jun 17;24(7):102736. doi: 10.1016/j.isci.2021.102736. PMID: 34278252; PMCID: PMC8261674.

[27] Prakashan D, P R R, Gandhi S. A Systematic Review on the Advanced Techniques of Wearable Point-of-Care Devices and Their Futuristic Applications. Diagnostics (Basel). 2023 Feb 28;13(5):916. doi: 10.3390/diagnostics13050916. PMID: 36900059; PMCID: PMC10001196.

[28] D. Citterio, T. R. L. C. Paixão, and W. R. de Araujo, "Introduction to paper-based point-of-care diagnostics," in Paper-Based Sensors, Wiley-VCH, Weinheim, Germany, 2018.

[29] C. Gonzalez-Solino, E. Bernalte, C. Bayona Royo, R. Bennett, D. Leech, and M. Di Lorenzo, "Self-powered detection of glucose by enzymatic glucose/oxygen fuel cells on printed circuit boards," ACS Applied Materials & Interfaces, vol. 13, no. 23, pp. 26704–26711, Jun. 2021, doi: 10.1021/acsami.1c02747.

[30] Gao, ZD., Qu, Y., Li, T. et al. Development of an Amperometric Glucose Biosensor Based on Prussian Blue Functionalized TiO_2 Nanotube Arrays. Sci Rep **4**, 6891 (2014). doi.10.1038/srep06891

[31] Baumbauer, C.L., Anderson, M.G., Ting, J. et al. Printed, flexible, compact UHF-RFID sensor tags enabled by hybrid electronics. Sci Rep **10**, 16543 (2020). doi.10.1038/s41598-020-73471-9

[32] H. Lu, M. Behm, S. Leijonmarck, G. Lindbergh, and A. Cornell, "Flexible paper electrodes for Li-ion batteries using low amount of TEMPO-oxidised cellulose nanofibrils as binder," ACS Applied Materials & Interfaces, vol. 8, no. 28, pp. 18097–18106, Jul. 2016, doi: 10.1021/acsami.6b05016.

[33] L. Hu, H. Wu, F. La Mantia, Y. Yang, and Y. Cui, "Thin, flexible secondary Li-ion paper batteries," ACS Nano, vol. 4, no. 10, pp. 5843–5848, Oct. 2010, doi: 10.1021/nn1018158.

[34] Mehta, D., Siddiqui, M. F. H., & Javaid, A. Y. (2018). Facial Emotion Recognition: A Survey and Real-World User Experiences in Mixed Reality. Sensors, 18(2), 416. doi.10.3390/s18020416

[35] N. Gautam, R. Verma, R. Ram, J. Singh, and A. Sarkar, "Development of a biodegradable microfluidic paper-based device for blood–plasma separation integrated with non-enzymatic electrochemical detection of ascorbic acid," Talanta, vol. 266, p. 125019, 2024, doi: 10.1016/j.talanta.2023.125019

INTERNATIONAL JOURNAL FOR RESEARCH

IN APPLIED SCIENCE & ENGINEERING TECHNOLOGY

Call : 08813907089 (24*7 Support on Whatsapp)